A MODIFIED PHASE SPACE MODEL AND ITS APPLICATION IN FITTING EFFECTIVE MASS DISTRIBUTIONS IN MANY-BODY REACTIONS

By S. Otwinowski

Institute of Nuclear Research, Warszawa*

(Received October 9, 1968)

A modified phase space model with a matrix element depending on baryon momentum is presented for πp interactions. The predictions of the model are shown to agree with the experimental effective mass distributions of pionic subsystems in the reactions $\pi^+ p \to p\, 5\pi$ and $\pi^+ p \to p\, 6\pi$ at 8 GeV/c. The production of mesonic resonances is estimated.

1. Introduction

An attempt is presented to describe pion production in the many-body processes at high energy. The analysis is based on a sample of $\pi^+ p$ interactions at 8 GeV/c with a nucleon and k pions in the final state [1]:

$$\pi^+ p \to p\, \pi^+ \pi^+ \pi^+ \pi^- \pi^-, \qquad k = 5 \tag{1}$$

$$\pi^+ p \to p\, \pi^+ \pi^+ \pi^+ \pi^- \pi^- \pi^0, \quad k = 6 \tag{2}$$

$$\pi^+ p \to n\, \pi^+ \pi^+ \pi^+ \pi^+ \pi^- \pi^-, \; k = 6. \tag{3}$$

The number of events collected in channels (1)–(3) and the corresponding cross-sections are given in Table I.

TABLE I

Channel	Number of events	Cross-section (mb)
$\pi^+ p \to p\pi^+\pi^+\pi^+\pi^-\pi^-$	504	0.40 ± 0.03
$\pi^+ p \to p\pi^+\pi^+\pi^+\pi^-\pi^-\pi^0$	1075	0.84 ± 0.06
$\pi^+ p \to n\pi^+\pi^+\pi^+\pi^+\pi^-\pi^-$	425	0.33 ± 0.04

* Address: Instytut Badań Jądrowych, Zakład Fizyki Wysokich Energii, Warszawa, ul. Hoża 69, Polska.

The differential cross-section can be written as a product of the two factors: of the average square of an unknown matrix element M describing the dynamics of the interaction, and of the phase space factor Φ:

$$P = |M|^2 \Phi.$$

Experimental data indicate that in the interactions discussed here statistical features of particle production are important. Therefore, the interaction probability depends significantly on the phase space factor Φ. The analysis of the difference between the phase space predictions and the experimental data may lead to suitable dynamic assumptions concerning the matrix element M.

In this paper a modified phase space model based on a simple dynamic assumption is presented and compared with the experiment.

2. *Comparison of the experimental data with the phase space predictions*

As a first step the relativistic phase space model (M = constant) was assumed and its predictions were compared with the experiment.

In Figs 1–29 experimental invariant mass distributions of various numbers of pions from 2 to k for all charge configurations in reactions (1) and (2) are presented. The dotted lines are the phase space curves, the reflections of pionic resonances having been taken into account — see Section 4. A significant disagreement is observed: the phase space curves are systematically shifted towards higher mass values with respect to the experimental mass distributions. The greater the number of pions in the considered subsystem the bigger seems to be the shift. The strongest disagreement is observed for the mass distribution of the system of all (k) pions (Figs 9, 29). The latter distribution is equivalent to the proton momentum spectrum in c. m. system, and the observed shift means that protons are emitted with c. m. momenta higher than predicted by the phase space model. Moreover, the angular

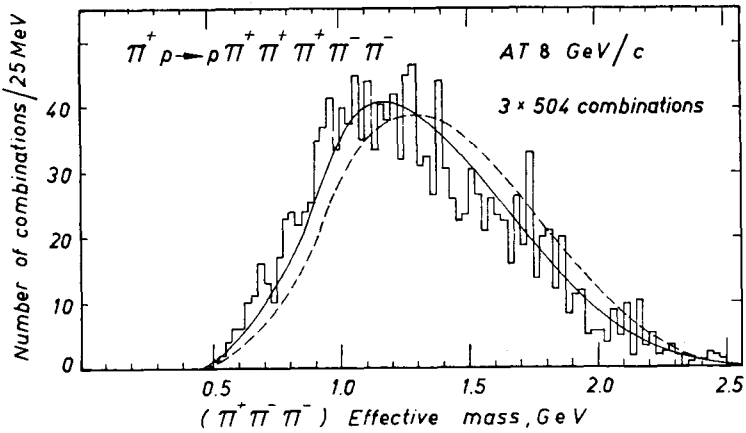

Fig. 1. ($\pi^+\pi^+$) effective mass distribution for reaction (1). In all figures presented in the paper dotted lines are the relativistic phase space predictions and continuous lines represent the modified phase space curves

ACTA PHYSICA POLONICA Vol. XXXV (1969) Fasc. 4

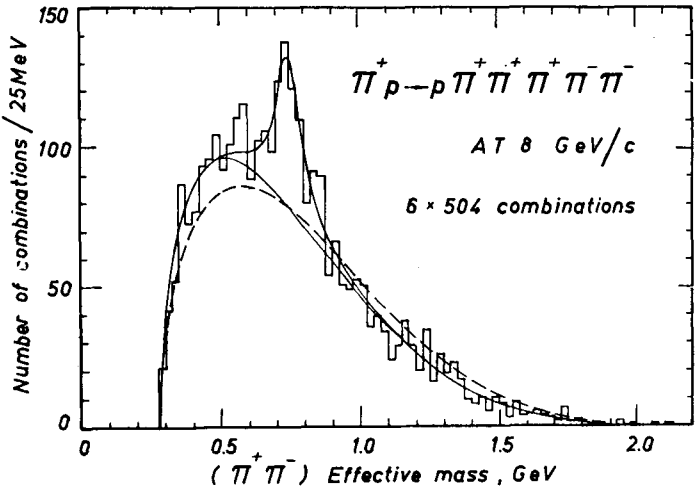

Fig. 2. $(\pi^+\pi^-)$ effective mass distribution for reaction (1). The continuous line is the sum of the modified phase space background and the Breit-Wigner curve of the ϱ^0 meson fitted to the experimental histogram

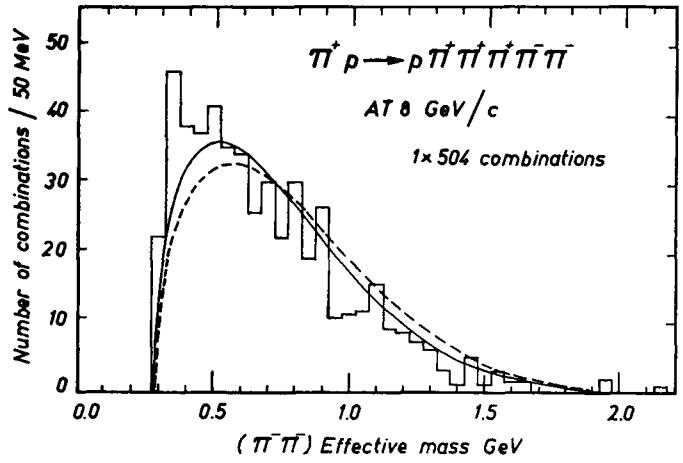

Fig. 3. $(\pi^-\pi^-)$ effective mass distribution for reaction (1)

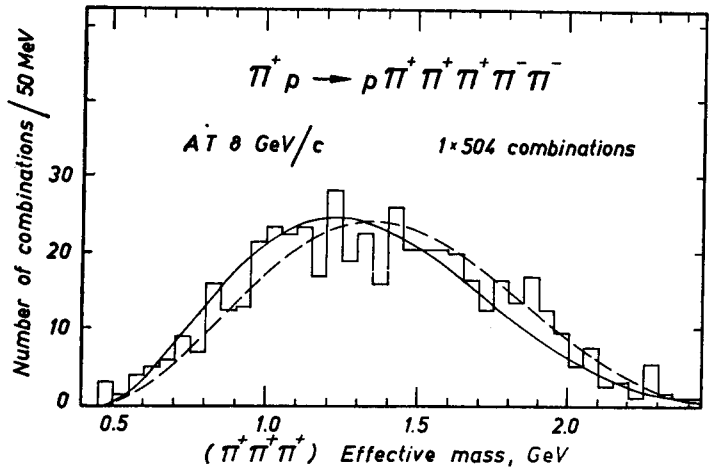

Fig. 4. $(\pi^+\pi^+\pi^+)$ effective mass distribution for reaction (1)

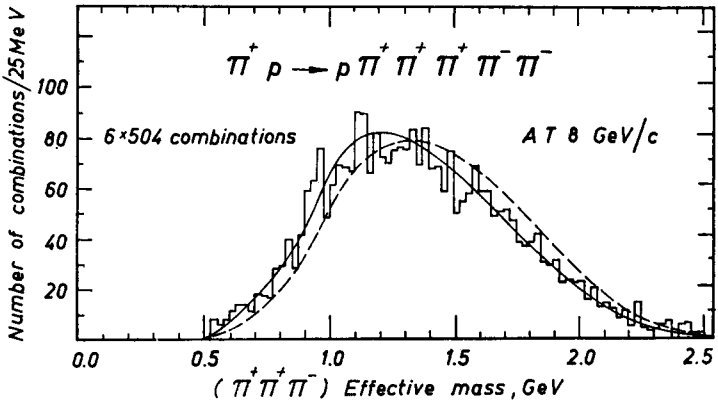

Fig. 5. $(\pi^+\pi^+\pi^-)$ effective mass distribution for reaction (1)

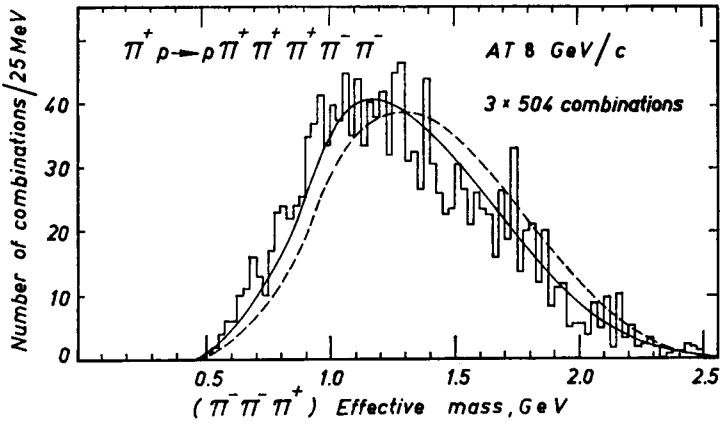

Fig. 6. $(\pi^-\pi^-\pi^+)$ effective mass distribution for reaction (1)

ACTA PHYSICA POLONICA Vol. XXXV (1969) Fasc. 4

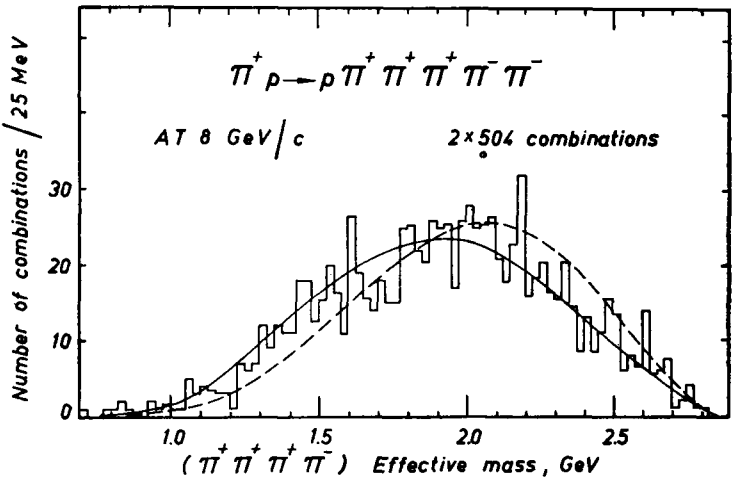

Fig. 7. ($\pi^+\pi^+\pi^+\pi^-$) effective mass distribution for reaction (1)

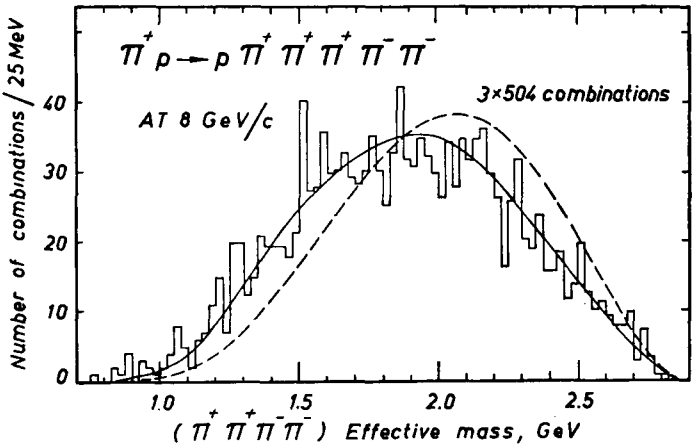

Fig. 8. ($\pi^+\pi^+\pi^-\pi^-$) effective mass distribution for reaction (1)

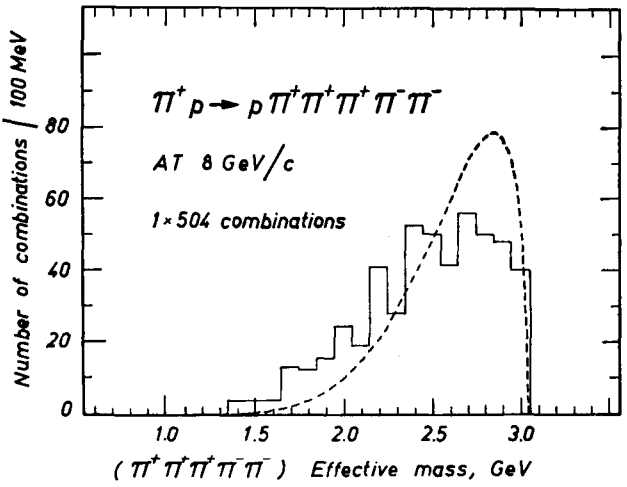

Fig. 9. ($\pi^+\pi^+\pi^+\pi^-\pi^-$) effective mass distribution for reaction (1)

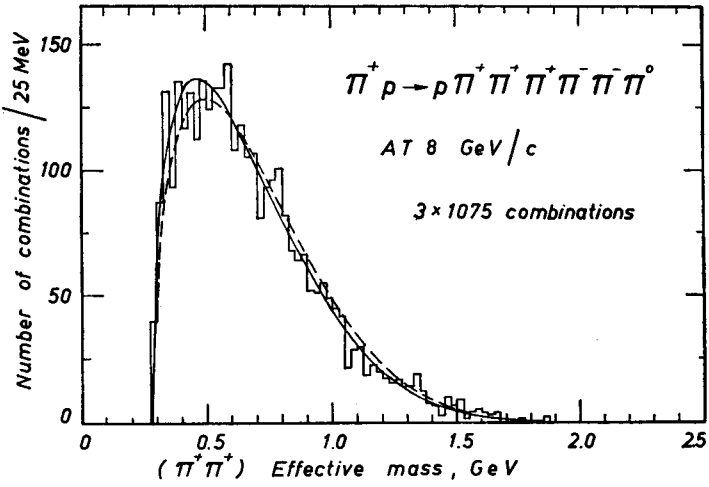

Fig. 10. $(\pi^+\pi^+)$ effective mass distribution for reaction (2)

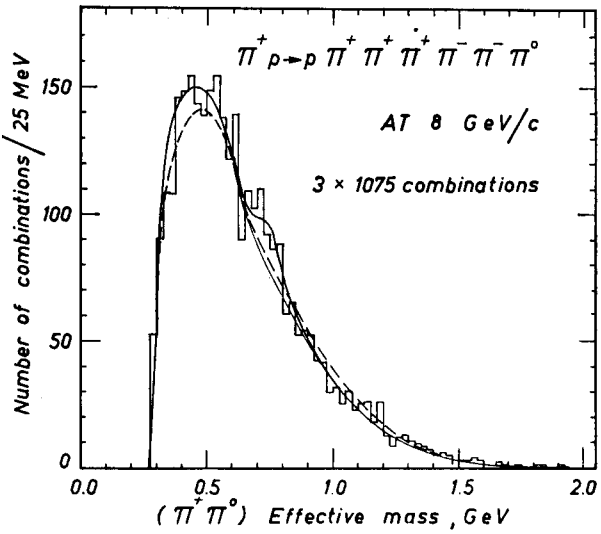

Fig. 11. $(\pi^+\pi^0)$ effective mass distribution for reaction (2). The continuous line is the sum of the modified phase space background and the Breit-Wigner curve for the ϱ^+ meson fitted to the experimental histogram

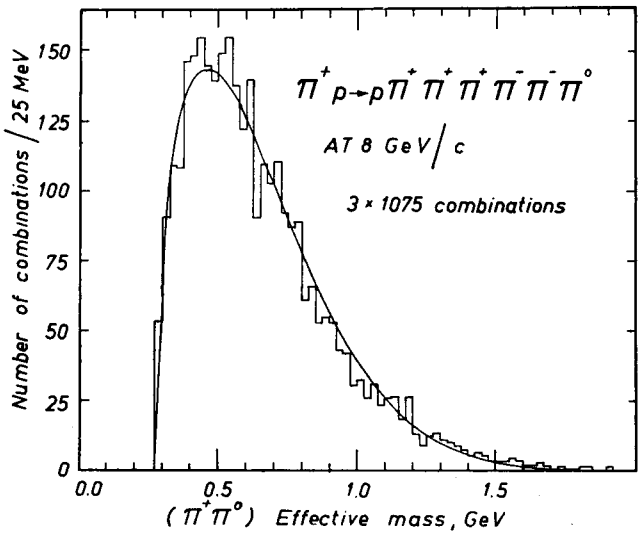

Fig. 11.*a* ($\pi^+\pi^0$) effective mass distribution for reaction (2). The continuous line is the modified phase space curve without resonance reflexions

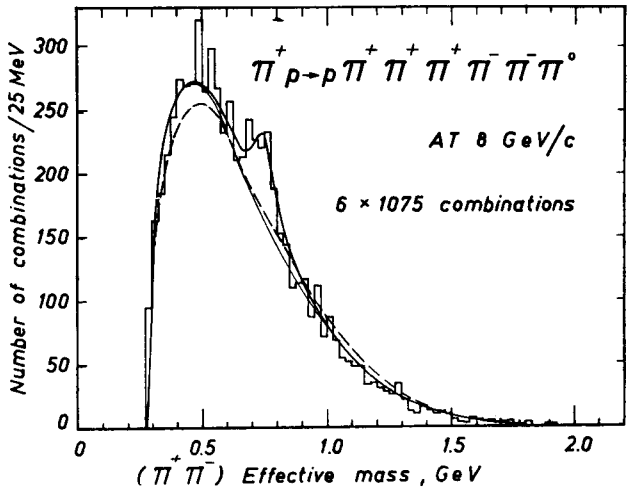

Fig. 12. ($\pi^+\pi^-$) effective mass distribution for reaction (2). The continuous line is the sum of the modified phase space background and the Breit-Wigner curve for the ϱ^0 meson fitted to the experimental histogram

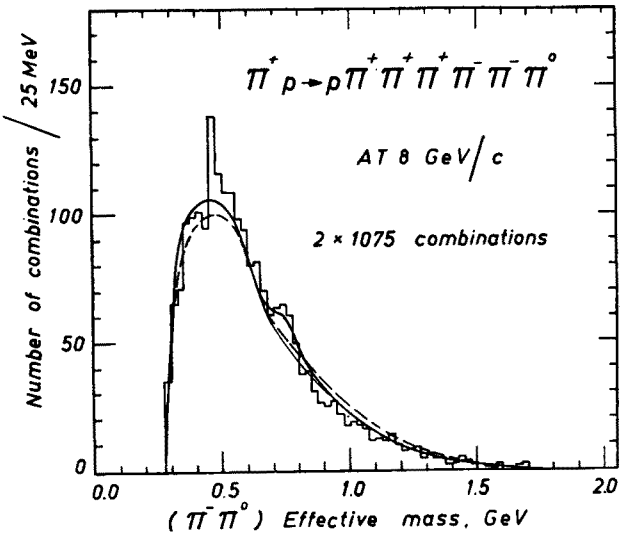

Fig 13. ($\pi^-\pi^0$) effective mass distribution for reaction (2). The continuous line is the sum of the modified phase space background and the Breit-Wigner curve for the ϱ^- meson fitted to the experimental histogram

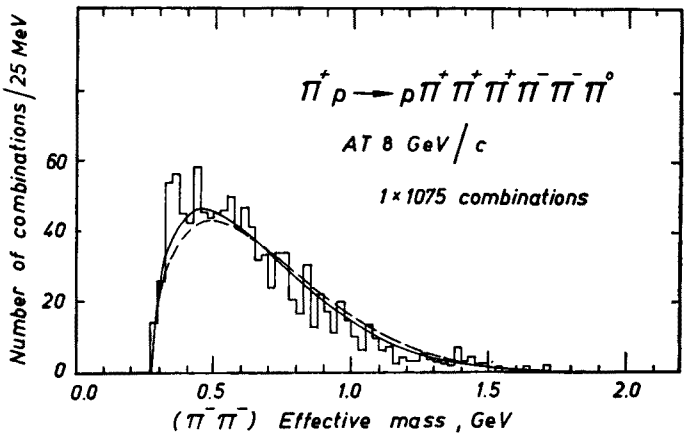

Fig. 14. ($\pi^-\pi^-$) effective mass distribution for reaction (2)

ACTA PHYSICA POLONICA Vol. XXXV (1969) Fasc. 4

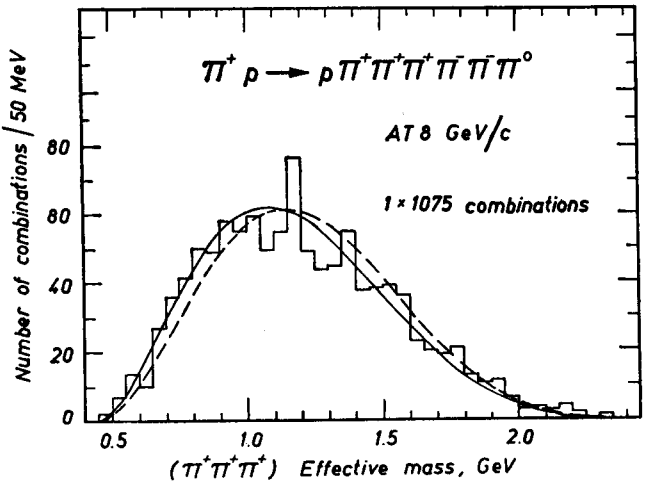

Fig. 15. $(\pi^+\pi^+\pi^+)$ effective mass distribution for reaction (2)

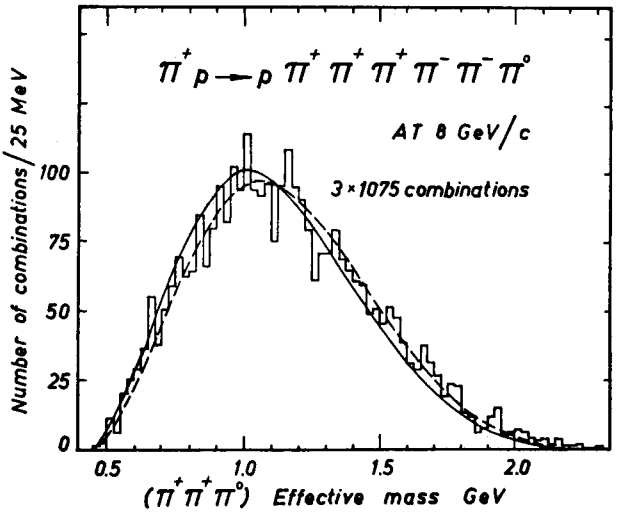

Fig. 16. $(\pi^+\pi^+\pi^0)$ effective mass distribution for reaction (2)

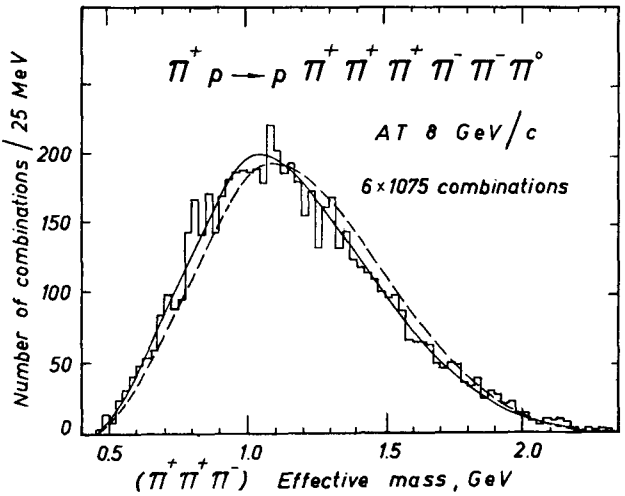

Fig. 17. $(\pi^+\pi^+\pi^-)$ effective mass distribution for reaction (2)

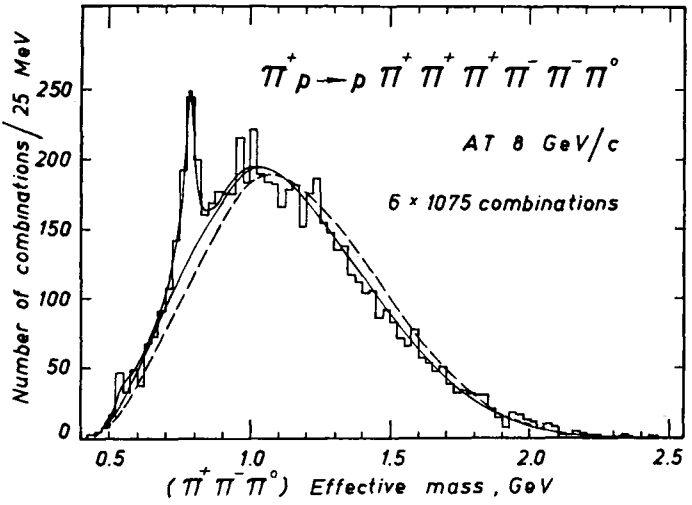

Fig. 18. $(\pi^+\pi^-\pi^0)$ effective mass distribution for reaction (2). The continuous line is the sum of the modified phase space background and the Breit-Wigner curves for the ω^0 and η^0 mesons fitted to the experimental histogram

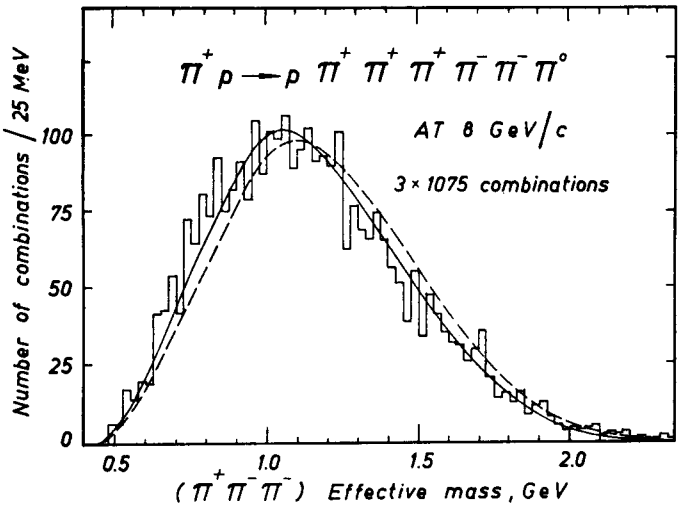

Fig. 19. $(\pi^+\pi^-\pi^-)$ effective mass distribution for reaction (2)

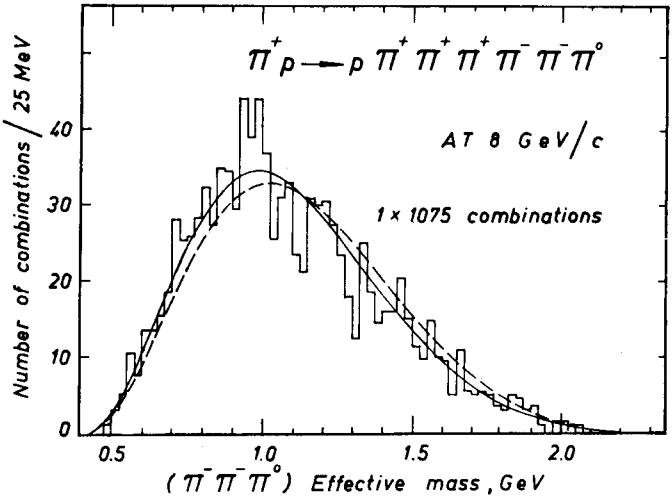

Fig. 20. $(\pi^-\pi^-\pi^0)$ effective mass distribution for reaction (2)

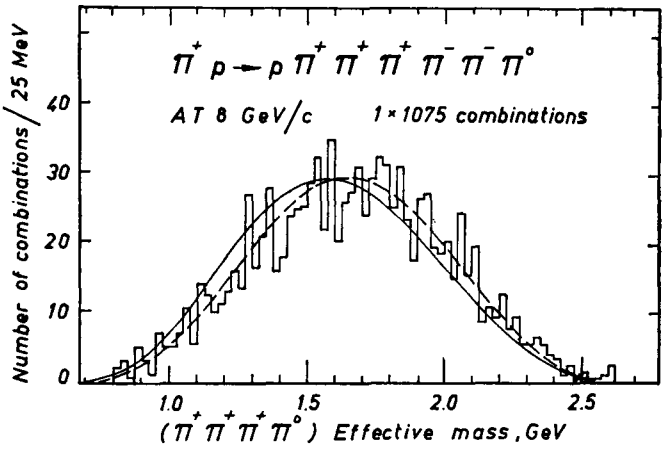

Fig. 21. $(\pi^+\pi^+\pi^+\pi^0)$ effective mass distribution for reaction (2)

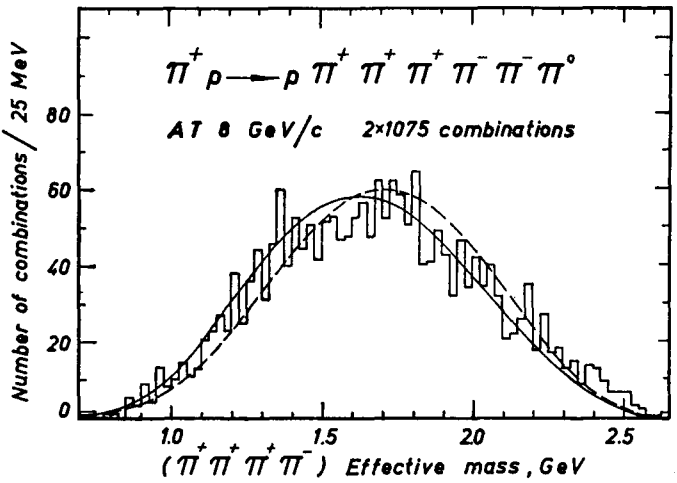

Fig. 22. $(\pi^+\pi^+\pi^+\pi^-)$ effective mass distribution for reaction (2)

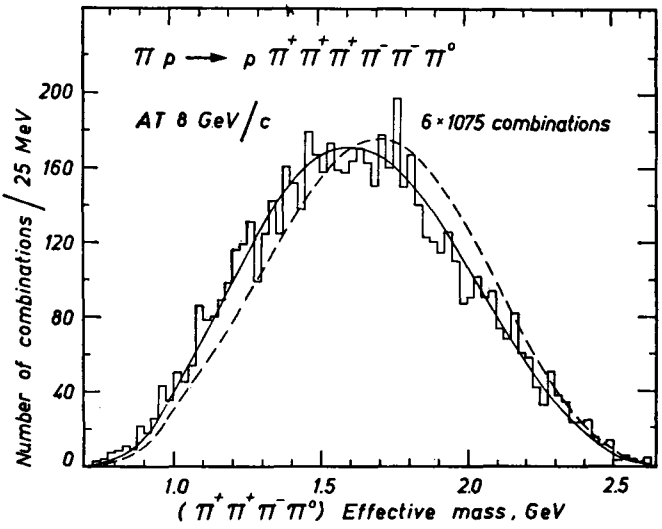

Fig. 23. ($\pi^+\pi^+\pi^-\pi^0$) effective mass distribution for reaction (2)

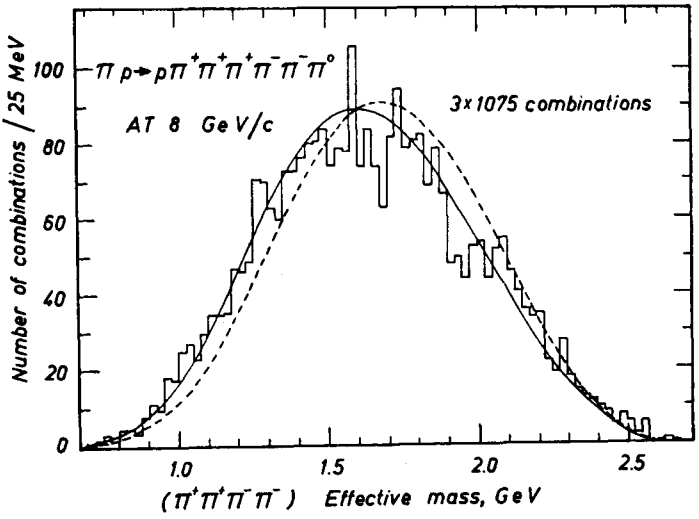

Fig. 24. ($\pi^+\pi^+\pi^-\pi^-$) effective mass distribution for reaction (2)

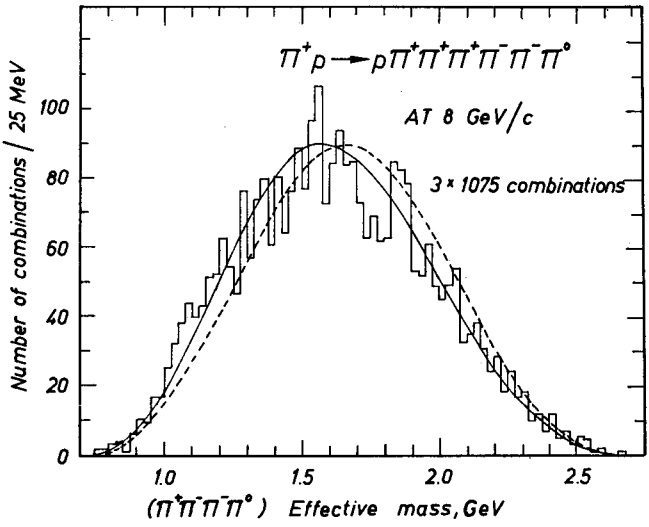

Fig. 25. $(\pi^+\pi^-\pi^-\pi^0)$ effective mass distribution for reaction (2)

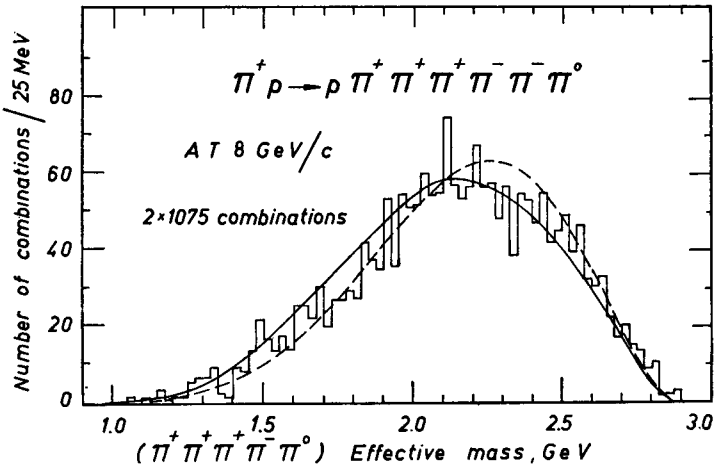

Fig. 26. $(\pi^+\pi^+\pi^+\pi^-\pi^0)$ effective mass distribution for reaction (2)

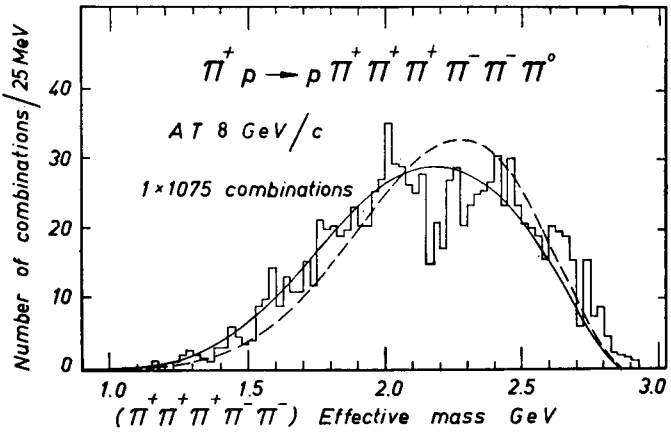

Fig. 27. $(\pi^+\pi^+\pi^+\pi^-\pi^-)$ effective mass distribution for reaction (2)

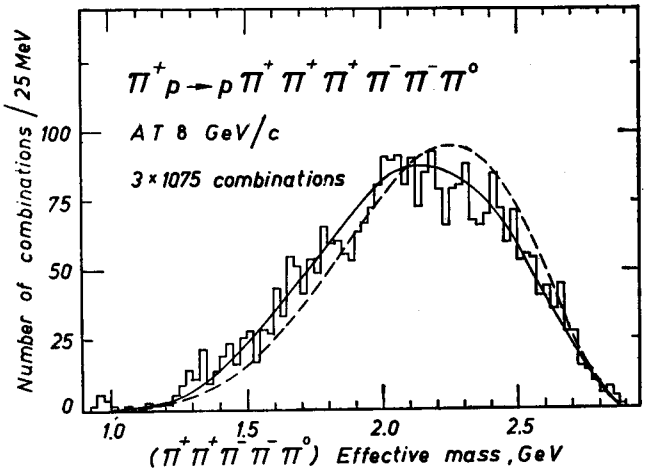

Fig. 28. $(\pi^+\pi^+\pi^-\pi^-\pi^0)$ effective mass distribution for reaction (2)

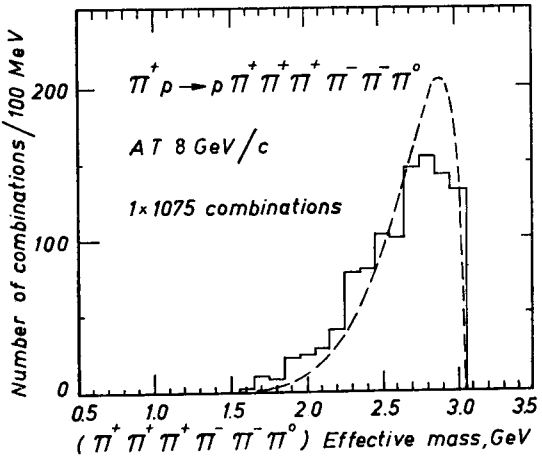

Fig. 29. $(\pi^+\pi^+\pi^+\pi^-\pi^-\pi^0)$ effective mass distribution for reaction (2)

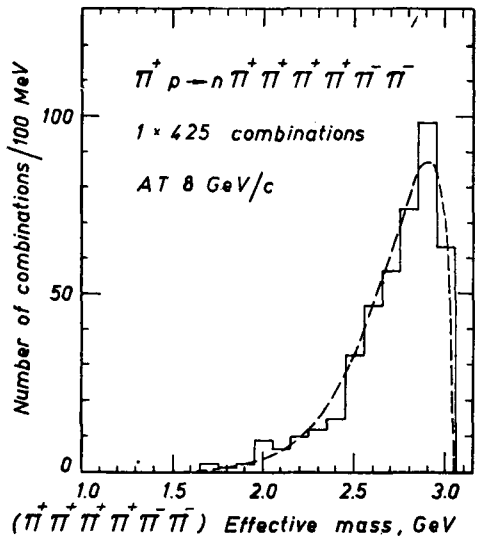

Fig. 30. $(\pi^+\pi^+\pi^+\pi^+\pi^-\pi^-)$ effective mass distribution for reaction (3)

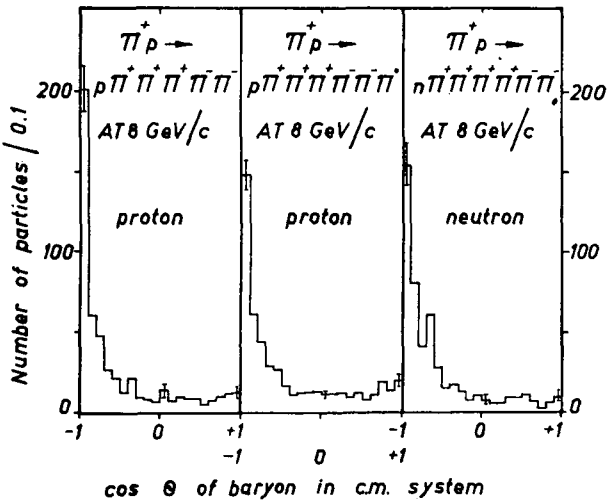

Fig. 31. Angular distribution of baryon in the c. m. system. The distributions are normalized to the same area

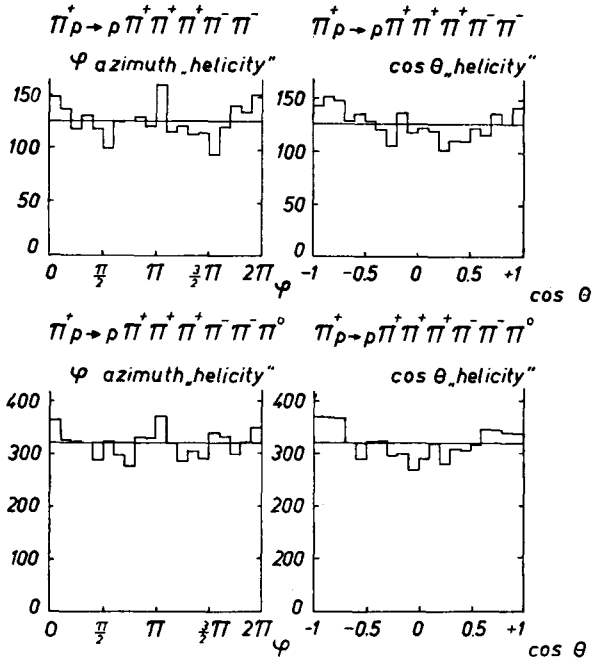

Fig. 32. Angular distribution of pions in the rest frame of the system of all pions for reaction (1) and (2). θ is the angle between the direction of the outgoing pion and the vector k opposite to the direction of the outgoing proton. φ is the azimuthal angle in the plane perpendicular to k measured from the reaction plane

distribution of protons in the c. m. system is strongly peaked backwards (Fig. 31). These facts suggest that the observed disagreement with the phase space model results mainly from the behaviour of protons.

3. The modified phase space model

Let us assume that the matrix element M depends only on the c. m. momentum of the baryon and consequently the phase space model remains valid within the pionic system. This approach will be called the modified phase space model.

Since the dependence of the matrix element on baryon momentum is unknown, the c. m. momentum distribution of baryons is taken from experiment.

The experimental distribution of the total energy of a k pion system (Figs 9, 29, 30) is in disagreement with the ordinary phase space predictions in channels (1) and (2), whereas in channel (3) the agreement is quite good. Therefore the modified phase space calculations were performed only for channels (1) and (2).

An immediate consequence of the modified phase space model is the isotropy of pion emission in the rest frame of the pionic system. This prediction, compared in Fig. 32 with experimental angular distributions in channels (1) and (2), is not inconsistent with the experimental data.

ACTA PHYSICA POLONICA Vol. XXXV (1969) Fasc. 4

In the next sections more detailed predictions of the model are tested against experimental invariant mass distributions of various pionic subsystems.

The N^* production has been neglected to simplify the calculations. It is considered that it does not bias strongly the results since the momenta of protons from the N^* decay are similar to those of protons produced directly.

4. Method of calculation

The aim of the calculation is to find the distributions of invariant mass of pionic subsystems, predicted by the modified phase space model.

The relativistic phase space model was applied to the system of k pions to calculate the mass distribution of a given subsystem at several values of the total energy of k pions in steps of 100 MeV. Every distribution was normalized to the experimental frequency of the corresponding energy of k pions and then all the contributions were summed up.

The phase space calculations were performed for the final state consisting of pions only and also for the final states including resonances: ϱ^0 in channel (1) and ϱ^0, ϱ^+, ϱ^-, ω^0, η^0 in channel (2). The experimental widths of the resonances were taken into account. Relative frequencies of various final states were estimated from the experiment.

In our calculation of the invariant mass distribution of a pionic subsystem the contributions from the final states with resonances were included if all pions from the resonance decay were either inside or outside the considered subsystem. Moreover, in the case of ω^0 or η^0 production, the reflections due to two out of three pions from the $\omega(\eta)$ decay were included.

As a result the invariant mass distributions predicted by the modified phase space model were obtained.

In pionic subsystems where the resonance peaks are observed the sum of the calculated mass distribution and the Breit-Wigner curve was fitted to the experimental histogram. In the fit to the ϱ production the relativistic Breit-Wigner formula with mass-dependent width [2] was used, whereas for the ω^0 and η^0 mesons the nonrelativistic Breit-Wigner formula was applied [3]. In cases of strong resonance production (ω^0 and ϱ^0) the mass, width and frequency were fitted; otherwise (*i. e.* for η^0 and $2^{\pm}$) the mass and width had to be kept fixed in the fit.

The shape of the calculated distributions depends significatly on the assumed frequencies of resonance production. Therefore the calculation of the reflections had to be repeated with improved values of the resonance parameters. Corrected distributions are compared with the experimental mass distributions in Section 5.

The presented method of calculation of resonance reflections was also used in the case of the ordinary phase space model and the same values of the resonance production rates were assumed.

5. Results

A. Comparison of the modified phase space model with the experiment

In Figs 1–8, 10–28 continuous lines are the modified phase space predictions. All of them are considerably shifted towards lower mass values with respect to the ordinary phase space curves; in consequence a fairly good agreement with experimental data was achieved.

ACTA PHYSICA POLONICA Vol. XXXV (1969) Fasc. 4

The consistency of both models with experimental data was estimated quantitatively by using χ^2 and Kolmogorov tests. The latter, concerned with integral distributions, is more efficient than the χ^2 test in detecting systematic deviations. The values of the confidence level calculated for all mass distributions are listed in Tables II and III for reactions (1) and (2), respectively.

TABLE II

Pionic system in reaction (1)	Confidence level (%)			
	Phase space		Modified phase space	
	χ^2	Kołmogorov	χ^2	Kołmogorov
$\pi^+\pi^+$	3	0.1	44	16
$\pi^+\pi^-$	10^{-3}	10^{-6}	28	93
$\pi^-\pi^-$	10^{-11}	10^{-6}	0.01	0.01
$\pi^+\pi^+\pi^+$	29	7	24	7
$\pi^+\pi^+\pi^-$	10^{-17}	10^{-16}	9	9
$\pi^+\pi^-\pi^-$	10^{-23}	10^{-19}	1	0.01
$\pi^+\pi^+\pi^+\pi^-$	10^{-8}	10^{-5}	67	7
$\pi^+\pi^+\pi^-\pi^-$	10^{-48}	10^{-23}	9	9
$\pi^+\pi^+\pi^+\pi^-\pi^-$	10^{-23}	10^{-13}	—	—

TABLE III

Pionic system in reaction (2)	Confidence level (%)			
	Phase space		Modified phase space	
	χ^2	Kołmogorov	χ^2	Kołmogorov
$\pi^+\pi^+$	0.02	0.2	4	57
$\pi^+\pi^-$	10^{-6}	10^{-7}	1	26
$\pi^+\pi^0$	13	4	21	71
$\pi^-\pi^-$	10^{-4}	10^{-6}	4	0.1
$\pi^-\pi^0$	1	10^{-3}	41	14
$\pi^+\pi^+\pi^+$	1	1	20	20
$\pi^+\pi^+\pi^-$	10^{-11}	10^{-12}	4	43
$\pi^+\pi^+\pi^0$	56	32	1	10^{-5}
$\pi^+\pi^-\pi^-$	10^{-11}	10^{-13}	4	1
$\pi^+\pi^-\pi^0$	0.1	0.1	5	77
$\pi^-\pi^-\pi^0$	0.1	10^{-4}	49	11
$\pi^+\pi^+\pi^+\pi^-$	10^{-4}	10^{-3}	0.1	1
$\pi^+\pi^+\pi^+\pi^0$	82	88	1	10^{-6}
$\pi^+\pi^+\pi^-\pi^-$	10^{-13}	10^{-12}	1	1
$\pi^+\pi^+\pi^-\pi^0$	10^{-48}	10^{-28}	1	11
$\pi^+\pi^-\pi^-\pi^0$	10^{-17}	10^{-14}	0.1	1
$\pi^+\pi^+\pi^+\pi^-\pi^-$	10^{-10}	10^{-4}	0.2	10^{-5}
$\pi^+\pi^+\pi^+\pi^-\pi^0$	0.1	0.1	0.1	10^{-5}
$\pi^+\pi^+\pi^-\pi^-\pi^0$	10^{-22}	10^{-15}	5	12
$\pi^+\pi^+\pi^+\pi^-\pi^-\pi^0$	10^{-21}	10^{-11}	—	—

ACTA PHYSICA POLONICA Vol. XXXV (1969) Fasc. 4

The conclusion is that the predictions of the ordinary phase space model are inconsistent with the data whereas the modified phase space model correctly reproduces most of the experimental distributions. The disagreement observed in some distributions seems to be related to an excess of low invariant masses of pairs of negative pions. The effect is reflected in complementary subsystems not containing negative pions. The mass distributions of these subsystems are shifted towards higher mass values.

In general the description of the data is satisfactory. It is to be stressed that the agreement has been achieved using a simple model in which one dynamical assumption is sufficient to describe the main features of particle production .The results presented here support this assumption, implying the dominant role of the proton in the interaction.

B. Resonance production

The invariant mass distributions calculated from the modified phase space model and the Breit–Wigner curves were used to fit the resonance production: ϱ^0 in channel (1), ω^0, η^0, ϱ^0, ϱ^+, ϱ^- in channel (2) — see Figs 2, 11, 12, 13, 18. The fitted curves (continuous lines) reproduce accurately the whole mass spectra.

The values of the mass, width, production rate and confidence level of the fit are given in Table IV. The mass and the width could be fitted only for resonances with a high production rate (ω^0 and ϱ^0); the results obtained are in good agreement with the generally accepted values. Therefore, the fit has been repeated using fixed mass and width in order to reduce the error of the production rate.

In fitting the resonance production with the ordinary phase space background a poor confidence level was obtained (see Table II and III). Moreover, the values of width and production rate were sometimes markedly different from those in Table IV. For example

TABLE IV

Resonance	Channel	Mass (MeV)	Width (MeV)	Number of events	Production rate (%)	Cross-section (μb)	Conf. level (%)
$\varrho^0 \to \pi^+\pi^-$	1	753.4±8.2	114±34	331±68	65.7±13.4	263±57	16
		756, fixed	115, fixed	334±42	66.3±8.3	265±39	28
$\varrho^0 \to \pi^+\pi^-$	2	749.3±8.9	107±37	398±91	37.3±8.5	313±75	1
		756, fixed	115, fixed	407±56	38.1±5.2	320±49	1
$\varrho^+ \to \pi^+\pi^0$	2	756, fixed	115, fixed	110±36	10.3±3.4	86±29	21
$\varrho^- \to \pi^-\pi^0$	2	756, fixed	115, fixed	68±28	6.3±2.7	53±23	41
$\omega^0 \to \pi^+\pi^-\pi^0$	2	783.7±3.7	45±8	329±43	30.8±4.0	288*±42	} 5
$\eta^0 \to \pi^+\pi^-\pi^0$	2	548.8, fixed	46, fixed	33±13	3.1±1.2	90*±35	
$\varrho^0 \to \pi^+\pi^-$	3	756, fixed	115, fixed	44±40	10.4±9.4	34±31	28

* Corrected for unseen decay modes according to UCRL — 8030 (August 1968).

a very broad ω^0 ($\Gamma = 75 \pm 10$ MeV) with a high production rate (54±5)% was found. Figs 2, 11, 12, 13, 18 show the background curves predicted by the ordinary phase space model (doted lines), normalized to the modified phase space background.

The discussed results show that the ordinary phase space model fails to describe our data. The approximation is too crude to allow for any reliable estimate of resonance production. A good knowledge of the background is of great importance in particular for high multiplicity processes where resonances, even if copiously produced, usually appear on a large background due to a large number of combinations. The description of the non-resonant background provided by the modified phase space model is remarkably consistent with the experimental mass distributions in the whole mass region. Therefore we feel fairly confident that our estimate of resonance production is correct and free of systematic errors.

In the calculation of the background shape a non-neglegible contribution comes from reflections of resonances. As an illustration of their importance the modified phase space background without any reflections, calculated for the $(\pi^+\pi^0)$ mass distribution, is presented in Fig. 11a. It is to be compared with the corresponding background including all reflections (continuous line in Fig. 11). The two curves lead to quite different estimates of the ϱ^+ production rate: the fit using the background with reflections gives $(10\pm3)\%$ of ϱ^+ production, whereas the other curve agrees with the experimental histogram thus suggesting that ϱ^+ is not produced at all.

6. *Conclusions*

It has been shown that in the π^+p interactions of intermediate multiplicity at 8 GeV/c statistical features of particle production are evident and baryon emission plays a dominant role in the dynamics of the interaction.

A simple phenomenological model was proposed and shown to reproduce correctly the main features of pion production. The model proved to be a useful tool to study resonance production by providing a presice description of the background.

One may expect that although the ordinary phase space model fails to describe the emission of all secondaries it might still be valid within a suitably chosen subsystem of particles of considerably reduced total energy. It would be interesting to see whether similar low energy statistical clusters can also be detected in other many-body reactions, for example in $p-p$ or $K-p$ collisions.

We are grateful to the CERN Track Chamber Division for providing us with films.

We are indebted to Professor M. Danysz and Drs M. Bardadin-Otwinowska, L. Michejda and R. Sosnowski for constant encouragement, helpful discussions and critical comments. We wish to thank Dr A. Wróblewski for reading the manuscript and comments.

It is a pleasure to record the efforts of our scanning and measuring staff.

REFERENCES

[1] T. Hofmokl, L. Michejda, S. Otwinowski, R. Sosnowski, M. Szeptycka, W. Wójcik and A. Wróblewski, *Nuclear Phys.*, **B4**, 573 (1968).

[2] J. D. Jackson, *Nuovo Cimento*, **34**, 1644 (1964).

[3] If the observed width of a resonance is large compared to its natural width, the resulution function is better approximated by a Breit-Wigner curve than by a Gaussian curve — private communication from L. Michejda.